ACS APPLIED ELECTRONIC MATERIALS

pubs.acs.org/acsaelm

Forum Article

Photolithographically Printed Flexible Silk/PEDOT:PSS Temperature Sensors

Sayantan Pradhan and Vamsi K. Yadavalli*

Cite This: *ACS Appl. Electron. Mater.* 2021, 3, 21−29

Read Online

ACCESS | Metrics & More | Article Recommendations | Supporting Information

ABSTRACT: Precise, real-time monitoring of temperature in flexible and bioconformable formats finds applications in healthcare and disease diagnostics. There is interest in the fabrication of biocompatible and biodegradable devices that can be safely resorbed inside the body or easily disposed of in the environment, reducing waste. Here, a fully organic, silk-protein-based temperature sensor is reported with attractive properties such as flexibility, transparency, conformability, durability, and biodegradability together with high sensitivity and accuracy. The sensor is composed of a flexible, photoactive silk fibroin substrate, on which interdigitated electrodes are photolithographically micropatterned using a photoactive silk sericin−PEDOT:PSS conductive ink. A temperature sensitive layer comprising photoactive silk sericin and rGO is integrated on the electrodes. Finally, the sensor is sheathed in a fibroin layer to eliminate interference from humidity. The sensor exhibits a high sensitivity of −0.99% °C^{-1} in the temperature range of 20−50 °C along with excellent stability in humidity from 10 to 90% RH. It possesses high cycling stability over multiple heating/cooling cycles. These layers are covalently integrated, improving mechanical stability and the retention of electrochemical behavior under deformation. The sensor is shown for the monitoring of surface temperature, including rapid measurement of skin temperature with accuracy. Finally, the temperature sensor is able to effectively degrade over a period of ∼10 days under proteolytic conditions. Such sensors have potential in personalized healthcare monitoring devices, improving efficient disease detection and diagnosis.

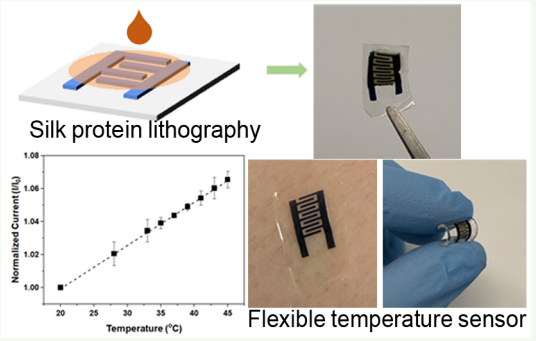

KEYWORDS: *flexible, temperature sensor, degradable, silk, PEDOT:PSS*

INTRODUCTION

There is increasing interest in exploring (bio)degradable materials for device fabrication for applications in regenerative medicine, implantable electronics, and human−machine interfaces. Such materials can provide added functionality including biocompatibility while potentially addressing problems pertaining to sustainability and electronic waste.[1−4] In such systems, various (bio)degradable, compostable, and dissolvable components can break down at controlled rates either via hydrolysis or biochemical reactions, with benign end products. They may be applied both in terms of external devices that can be safely discarded in the environment, or for *in vivo* implantation, in which the need for extractive surgeries to recover the device is obviated.[5] Applications range from resorbable diagnostic or therapeutic medical devices[6,7] to environmental monitoring[8] and security systems.[9]

Among the diverse biointegrated and wearable systems that have been studied, the measurement of local temperature is an essential parameter in the monitoring of physiological function.[10] Of interest have been flexible and conformable temperature sensors that can function as wearables for real-time healthcare monitoring.[11,12] While rigid thermometers have long been in existence, creating direct contact with the body has the potential to provide localized, real-time, or continuous sensing or improve comfort and accuracy. To accomplish conformal contact with uneven and dynamic interfaces, soft, flexible, conformable, and biocompatible sensors have been proposed. Skin has been a primary target,[13−15] whereas localized temperature recordings for monitoring soft tissue interfaces for wound healing, or cardiovascular or pulmonary function, may also be envisioned for disease diagnosis or observing organ function.[16]

The demand for improved, degradable, and conformable sensors continues to motivate research in this field toward ubiquitous sensing.[17,18] The properties of a flexible temperature sensor may be affected by complex strains/stresses induced by the body. Thus, the presence of skin-like conformability and stretchability is desirable. In addition to conferring degradability, properties such as lightweight,

Special Issue: Wearable and Biodegradable Sensors

Received: November 18, 2020
Accepted: December 6, 2020
Published: December 17, 2020

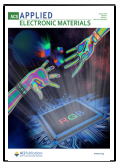

https://dx.doi.org/10.1021/acsaelm.0c01017
ACS Appl. Electron. Mater. 2021, 3, 21−29

thinness, and mechanical flexibility are desirable for improved conformability and comfort. They can promote accurate sensing at tissue interfaces or for packaging and smart textile applications. Further, sensors capable of operating in wet and dry environments are needed. A challenge lies in providing stable and reliable operation with properties intact for designed operational periods, followed by their degradation. Finally, integration with fabrication techniques makes the devices accessible and easily reproducible at low cost.

There have been prior reports of such flexible sensors for temperature measurement, which operate via different mechanisms (e.g., resistive, capacitive, or thermocouple) or different materials (e.g., carbon-based, metals, or conducting polymers), on a variety of substrates (e.g., polyimide (PI), polydimethylsiloxane (PDMS), polyurethane (PU), polyethylene terephthalate (PET)-based films, paper, or textiles).[11,13,19,20] Among various conducting inks that have been reported, conducting polymers such as poly(3,4-ethylenedioxythiophene):polystyrenesulfonate (PEDOT:PSS) or polyaniline (PANI) are attractive for the development of flexible and wearable devices (Table 1).[21] Many sensors

Table 1. Some Recent Comparative Reports of Temperature Sensors Indicating the Temperature Coefficient of Resistance (TCR) Response

active material	temperature range (°C)	TCR	reference
PEDOT:PSS + GOP sensing layer on Ag electrode	25−50	−0.77% $°C^{-1}$	26
PBH−rGO composite	20−65	−0.3% $°C^{-1}$ to −0.8% $°C^{-1}$	14
rGO	25−45	−1.30% $°C^{-1}$	15
silk fibroin and Ca (II) ions	0−40	−1.9% $°C^{-1}$	28
silk-based graphitic nanocarbon	25−80	−0.81% $°C^{-1}$	29
Gr/SF/Ca^{2+}	20−50	−2.1%$°C^{-1}$	51
PEDOT:PSS	30−55	−0.42% $°C^{-1}$	52
graphene/PEDOT:PSS	30−45	−0.064% $°C^{-1}$	24
PDMS/PEDOT:PSS/rGO	30−50	−1.69% $°C^{-1}$	53
silk/PEDOT:PSS	20−50	−0.99% $°C^{-1}$	this work

incorporate either nondegradable synthetic substrates and/or use metallic electrodes. For example, temperature sensors based on CNT ink and (PEDOT:PSS) solution were printed on PET.[22] A PEDOT:PSS sensing layer was sandwiched between two PDMS layers with sensors prestrained to improve sensitivity and linearity by creating microcracks.[23] A skin-conformable inkjet printed temperature sensor using graphene/PEDOT:PSS as the active material was shown with screen printed silver conductors and inkjet-printed graphene/PEDOT:PSS temperature sensors. The functional layer was printed on an adhesive bandage, which had a polyurethane surface and polyacrylate adhesive layer.[24] The negative effect of humidity on the electrochemical behavior of PEDOT:PSS motivated sensors with high humidity stability.[25] A fluorinated passivating polymer with low water permeability was used to provide stability to a cross-linked PEDOT:PSS sensing layer on Ag electrodes printed on a polyethylene naphthalate (PEN) substrate.[26] To date, fully degradable and mechanically flexible temperature sensors based on organic components have not been shown.

Natural biopolymers may provide an avenue for flexible temperature sensing with degradability.[2,27] In particular, silk proteins have been reported as ionotronic skins,[28] using silk fibroin and Ca(II) ions, or as e-skin by assembling a temperature and strain sensor using transparent silk-nanofiber-derived carbon fiber membranes.[29] A healable and multifunctional e-tattoo based on a graphene/silk fibroin/Ca^{2+} was shown to be responsive to environmental changes, such as strain, humidity, and temperature variation.[30] Here, for the first time, we demonstrate the photolithographic fabrication of a functional, flexible, and degradable temperature sensor using fully organic components. A room-temperature, aqueous "silk protein lithography" technique is used with photoreactive silk proteins as a route to multiscale fabrication.[31,32] A photoreactive silk fibroin sheet functions as a flexible, biocompatible substrate and a humidity protection layer, whereas functionality derives from conductive bioinks. These bioinks comprise the conducting polymer PEDOT:PSS mixed with photoreactive silk sericin, which allow facile fabrication into microelectrodes via photolithography. A silk sericin/reduced graphene oxide (rGO) ink is cross-linked as the electrochemical connector. The sensors are mechanically robust, thin, and ultralightweight while possessing humidity stability. The sensors are stable in both air and liquid environments over several days and can be stored in dry and wet conditions. The use of silk proteins to form novel degradable and biocompatible, yet functional (e.g., conducting) substrates provides a "green" future for tissue interfacing (bio)electronics and electronic skins.[33,3,34]

MATERIALS AND METHODS

Synthesis of Photoactive Silk Proteins. Biodegradable temperature sensors were formed using the previously reported method of silk protein lithography.[31,32] Photoreactive silk fibroin (photofibroin) was used as the substrate and protective sheath, and photoreactive sericin (photosericin) was used to form the photopatternable conducting ink. Synthesis was performed following protocols developed.[31,32] Briefly, the silk proteins (fibroin or sericin) were dissolved in 1 M LiCl in a DMSO solvent system and reacted with 2-isocyanatoethyl methacrylate in stoichiometric amounts at 60 °C under inert conditions for 5 h. The reaction mixture was precipitated in cold ethanol for 12 h. The product was washed 3 times in a 1:1 ratio of cold ethanol/acetone and lyophilized to obtain photoactive silk protein.

Formation of Conductive Composites. A photopatterning conducting ink for the fabrication of sensing microelectrodes was formed using a composite of the conducting polymer PEDOT:PSS with photosericin. The protein matrix forms a stable and biodegradable carrier that entraps the PEDOT:PSS while making it patternable using an aqueous process. The electrochemical characteristics, characterization, and patterning of this ink were earlier reported.[35] A 1% (w/w) dispersion of dry PEDOT:PSS pellets (Sigma-Aldrich, St. Louis, MO) in water was obtained by ultrasonicating for 30 min and filtering using a 0.25 μm syringe filter. DMSO (5%, v/v) was added to the dispersion to enhance its conductivity and stability. To form the conducting ink, photosericin was mixed with the PEDOT:PSS dispersion at varying concentrations, with appropriate amounts of an Irgacure 2959 photoinitiator to facilitate cross-linking.

A composite of a photoactive silk sericin and rGO was used to enhance conduction and sensing. GO was reduced to rGO chemically using an aqueous protocol.[36] Briefly, a 2 mg/mL solution of GO (University Wafer, South Boston, MA) was reduced at room temperature using L-ascorbic acid (5 mg per 1 mg of GO) for 1 h under continuous stirring. Reduction was verified by UV−vis. Freshly

https://dx.doi.org/10.1021/acsaelm.0c01017
ACS Appl. Electron. Mater. 2021, 3, 21−29

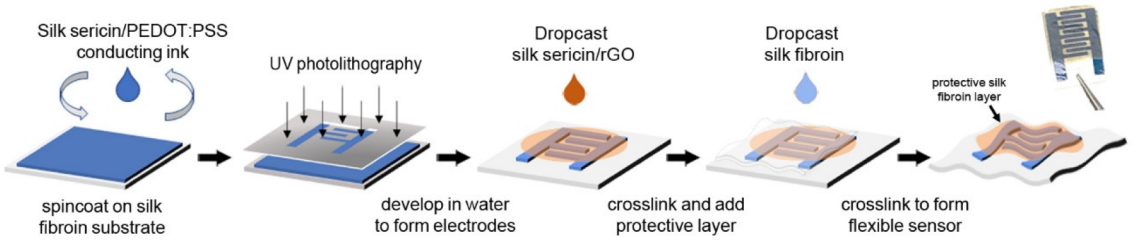

Figure 1. Schematic of the formation of a flexible silk/PEDOT:PSS temperature sensor.

prepared rGO was mixed with the photosericin at varying concentrations with PI added to the solution.

Fabrication of the Temperature Sensor. Microfabrication of the temperature sensor was carried out via contact photolithography using a benchtop setup (no cleanroom needed) (Figure 1). The substrate was prepared by casting a solution of 7.5% (w/v) photofibroin and 1.5% PI in formic acid on clean glass slides. The solution was dried under ambient conditions and cross-linked using an OmniCure S1000 UV Spot Curing lamp (Lumen Dynamics, Ontario, Canada) (365 nm UV (2 mW cm^{-2}) for 2 s) to form flexible substrates. Interdigitated electrodes (IDEs) were formed by spin-coating a solution of photosericin containing 28% (w/w) PEDOT:PSS and PI (0.2 μL/mg) on the substrates and drying under dark conditions in a fume hood. IDEs were patterned by cross-linking the ink under UV light for 2.5 s through a photomask, followed by developing in DI water. The temperature sensing layer was fabricated by casting a solution of 1% (w/w) of rGO and photosericin + PI on the IDEs and drying, followed by UV cross-linking. The top passivation layer was fabricated by casting a solution of 7.5% (w/v) photofibroin and PI in hexafluoro-2-propanol (HFIP, Sigma-Aldrich, St. Louis, MO) and cross-linking to form an integrated, flexible device.

Device Characterization and Temperature Sensing. To perform electrochemical experiments on the flexible silk temperature sensors, connections were made using copper wires. Measurements were performed using a Gamry Interface 1010E potentiostat (Gamry Instruments, Warminster, PA). Conductivity measurements on the sensors were calculated from $I-V$ scans performed in the range of −1 to 1 V at 50 mV s^{-1}. A water bath placed on a hot plate with a commercial thermocouple was used to control the temperature at which sensor measurements were taken. To obtain the conductivity at each temperature point, an $I-V$ scan was performed after equilibration for 5 min. Responses at different humidity were measured by placing the sensors in a humidity controlled desiccator. The sensor was maintained at each humidity level for 30 min before conductivity measurements were performed. For all calculations, room temperature (20 °C) was taken as initial temperature (T_0).

Real-time measurement of temperature was performed using chronoamperometry at a 1 V potential. A calibration plot was obtained using amperometric measurements (I vs t) by varying the temperature from 20 to 45 °C. The temperature was kept stable at each point for 50 s. Current values (I) were normalized to the value at 20 °C (I_0) to obtain a calibration curve. For the determination of the temperature of a surface, amperometric measurement was obtained at room temperature for 50 s followed by placing the sensor on the surface (with a fibroin substrate in contact with the surface) and taking a reading for 50 s. The final temperature was calculated from the calibration curve.

Degradation and Stability in Aqueous Media. The stability of the devices was observed by storage in PBS over extended period of time (several weeks) followed by electrochemical testing. Degradation of devices was observed under ezymatic conditions. Unsheathed devices (no top fibroin layer) were immersed in 3 mL of PBS solution containing 1 mg mL^{-1} of protease (Protease XIV from *Streptomyces griseus*, ≥3.5 U mg^{-1}, Sigma-Aldrich) and stored at 37 °C. A higher concentration of enzyme was used in comparison to representative studies[37,38] in order to speed up the process. A control set was designed with devices immersed in PBS buffer at 37 °C. To preserve enzyme activity, the solution was replaced every 2 days. Imaging was performed on the devices following removal from the enzyme solution and drying in a gentle N_2 stream.

RESULTS AND DISCUSSION

The proteins obtained from the silkworm, both silk fibroin and the glue-like protein sericin, possess a unique complement of properties that make them extremely suitable for applications in flexible and transient devices. These include processability as well as physical and biological properties including mechanical strength, optical transparency, biocompatibility, and biodegradability.[39−41] The ability to perform photolithography with chemically modified silk proteins further provides the benefit of scalable microfabrication. To fabricate a flexible temperature sensor, we take advantage of these properties together with the conductive polymer poly(3,4-ethylenedioxythiophene) polystyrene sulfonate (PEDOT:PSS).[21] The temperature sensitivity of PEDOT:PSS arises from the enhancement of charge carrier transport and generation of charge carriers under a thermal stimulus, which results in a decrease in resistance with increasing temperature.[42,43] The silk proteins therefore provide both the structural and functional components of the sensor.

Fabrication of Flexible Organic Temperature Sensors. In order to form the flexible, biodegradable temperature sensor, the various components were fabricated using silk protein photolithography. The modification of silk proteins with photo-cross-linkable moieties makes them compatible with a facile photolithographic process. The benchtop technique used in this work is scalable and can be used to repeatably pattern high-resolution microstructures over large areas (cm). Fibroin films thus formed have been previously reported as mechanically robust, biodegradable substrates.[44] High tensile strength (~100 MPa), optically transparency, and stability in physiological conditions makes them ideal for flexible and bioconformable devices.[45] The photoreactive, conducting ink formed from silk sericin and PEDOT:PSS is a versatile matrix for electrochemical sensing. The characterization of microelectrodes formed using this ink was earlier shown.[35] The photosericin helps to overcome the brittle nature of PEDOT:PSS films and improves stability. In this study, the temperature sensitivity of PEDOT:PSS was used as the transduction mechanism. Specifically, on applying a thermal stimulus, the charge transport carriers increase along with an increase in the number of charge carriers. This increase in carrier mobility decreases the resistance of the temperature sensor, which is reported as a function of temperature.[42,43]

The flexible substrates are formed as thin, smooth, mechanically robust silk fibroin films cross-linked on glass supports. The PEDOT:PSS ink was patterned on these substrates by spin-coating, followed by photolithography. The process schematic is shown in Figure 1. Interdigitated

https://dx.doi.org/10.1021/acsaelm.0c01017
ACS Appl. Electron. Mater. 2021, 3, 21−29

electrodes (IDEs) with a 250 μm finger width were fabricated to have a small form factor for the sensors (IDEs cover ~1 × 2 mm area on a substrate that is ~10 × 10 mm). The films were soaked in water for development and to delaminate them from the support and form free-standing devices (Figure 2a). A

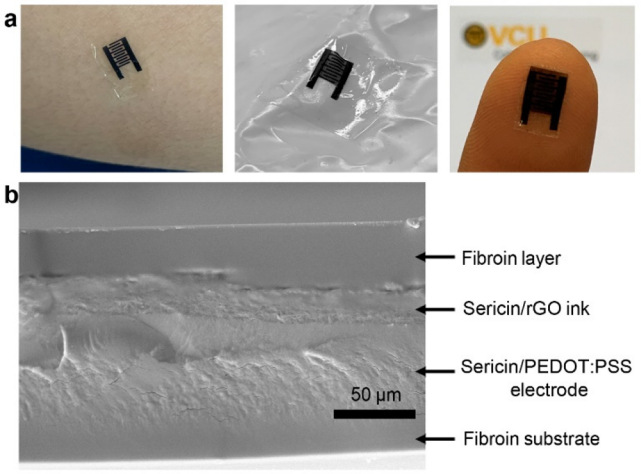

Figure 2. Images showing the flexible temperature sensor formed from silk proteins. (a) The sensor may be placed on skin or integrated into a wrinkled surface (e.g., a textile) with a small form factor. (b) SEM imaging of the cross section of the sensor showing the layers that are covalently integrated, preventing delamination and improving stability.

conducting composite of rGO and photosericin was cast on the electrodes and covalently cross-linked, taking advantage of the same pendant methacrylate moieties present in the substrate and electrodes to form interpenetrating layers.[31] rGO is used as the temperature sensing element due to its well-known phenomenon of temperature dependent charge transport behavior. Upon thermal excitation, the mobility of charge carriers in rGO increases, thus increasing the conductivity of the material. Finally, to provide stability against humidity, a fibroin layer was used to sheath the top of the sensor. The use of water as the developing solvent makes the entire process benign and environmentally friendly. The chemical cross-linking of the different layers using the same chemistry makes the entire device more robust and durable and less prone to failure under multiple mechanical deformations and flexure. By incorporating the PEDOT:PSS in the photosericin matrix, which contains residual methacrylate groups, the IDEs are covalently attached to the underlying fibroin substrate. Figure 2b shows an SEM image of the cross section of the device, showing how the layers are integrated. Additional images showing the well-integrated boundaries between the layers are shown in Figure S1.

Device Characterization and Optimization. The conductivity of the PS/PEDOT:PSS ink composite increases with PEDOT:PSS concentration in the composite. PEDOT:PSS (28%) was chosen to be the optimum concentration, which permits good electrochemical properties, together with the ability to form high-resolution electrodes via photolithography (e.g., at higher concentrations, the dark color of PEDOT:PSS reduces the fidelity of structures formed by UV cross-linking). In order to improve the electromechanical properties of the ink, 5% (v/v) DMSO was added to the PEDOT:PSS dispersion in water as a dopant. Linear voltammetry scans performed show a linear increase in current with an increase in potential. $I-V$ curves were obtained using a sensor with 1 wt.% rGO in the temperature sensitive layer while the temperature is varied from 20 to 50 °C (Figure S2). The experiment was conducted with a free-standing (unsupported) sensor suspended in a temperature-controlled water bath. The sensor response is obtained on the order of seconds. There is a linear decrease in resistivity upon increasing the temperature from 20 to 50 °C, which may be expressed in terms of increasing current (normalized to initial I_0) (Figure 3). The inset shows the change in signal as a

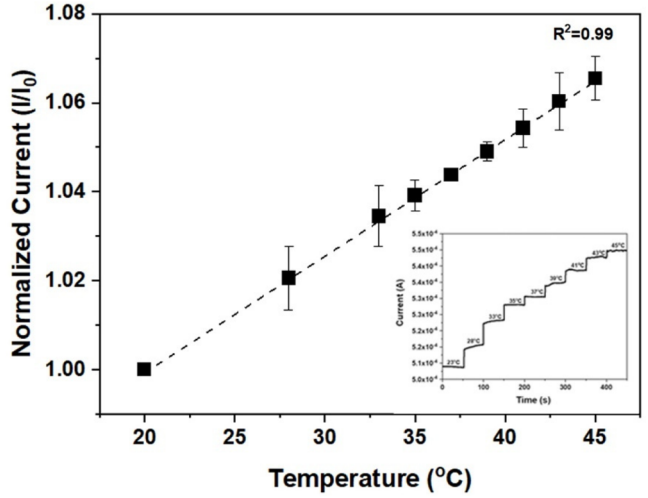

Figure 3. Calibration curve showing the temperature response of the flexible sensors. The inset shows the signal vs time measured by chronoamperometry in steps of 5 °C. (n = 3 different sensing experiments).

function of temperature over time. The resistivity at each temperature was calculated from the slope. The temperature sensitivity is expressed in terms of the temperature coefficient of resistance (TCR): TCR = $\frac{R-R_0}{R_0 * \Delta T}$*100. The TCR value of devices with 1% rGO in the conducting layer was calculated to be −0.99% °C^{-1}. This is very competitive in comparison to earlier reports, particularly noting that the device reported in this work is free of metals or conductive metal/metal oxides as charge collectors. The TCR values for some recently reported temperature sensors is shown in Table 1.

The temperature sensor reported here utilizes two different conducting composites: PS/rGO and PS/PEDOT:PSS. The inclusion of the (photoreactive) sericin offers a stable, patternable matrix for the rGO and PEDOT:PSS while also providing biodegradation under proteolysis. Both rGO and PEDOT:PSS have been used as the active sensing elements in temperature sensors.[14,26] Hence, the temperature sensitivity of each layer was separately investigated. The effect of temperature on the resistance of PS/PEDOT:PSS and PS/rGO was studied while the configuration (amount of material and area) was kept similar (Figure S3). The temperature sensitivity of the 1% rGO/PS layer (−1.51% °C^{-1}) is higher compared to the 28% PEDOT:PSS/PS layer (−0.86% °C^{-1}). In comparison to the individual composites, the TCR of the temperature sensor is −0.99% °C^{-1}. Although the change in resistance is not linear for either of the composites, the response of the final sensor is linear. Since the sensitivity of the 1% rGO/PS is

https://dx.doi.org/10.1021/acsaelm.0c01017
ACS Appl. Electron. Mater. 2021, 3, 21−29

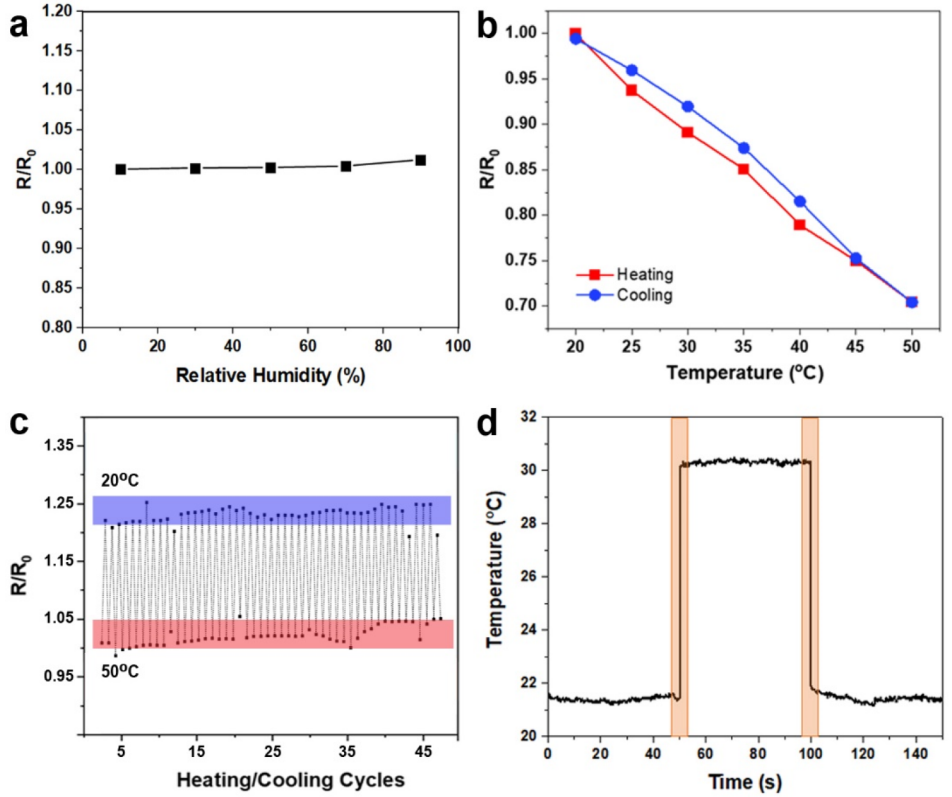

Figure 4. (a) Effect of humidity on a fibroin sheathed temperature sensor. (b) Measurement of TCR hysteresis of the sensor in a single heating and cooling cycle. (c) Repeated cycling between 20 and 50 °C. (d) Temporal sensor measurement of skin surface temperature (forearm).

higher than the 28% PEDOT:PSS/PS layer, it was used as the temperature sensitive layer.

To optimize device characteristics, we investigated the use of rGO dispersed within the IDEs instead of using it as a separate layer. The temperature sensitivity of electrodes with 1 wt.% rGO in the PS/PEDOT:PSS ink composite was estimated at −0.5% $°C^{-1}$, which is almost half the sensitivity of devices with 1% rGO in the top layer (−0.99% $°C^{-1}$) (Figure S4). Similarly, increasing the concentration of rGO in the top layer was studied. The temperature dependent $I-V$ characteristics of devices with varying rGO loading were obtained from 20 to 50 °C. Even though the overall resistivity of the devices decreased while the rGO concentration was increased from 1 to 3 wt.%, the temperature sensitivity of the devices decreased (Figure S5). This can be explained by the percolation threshold and dispersion of rGO in the photosericin (PS) matrix. PS/rGO (1%) is more efficiently dispersed, making it more sensitive to temperature changes. The charge carrier mobility of the PS/rGO composite might be impeded at higher temperatures with higher rGO loading. Hence, the configuration as shown in Figures 2 and 3 was proposed.

Temperature Response to Humidity. The change of conductivity depending on the environmental conditions such as humidity and temperature is important for device operation. The influence of relative humidity (RH) on the electrical and optical properties of PEDOT:PSS has been previously reported.[46] A significant cause of degradation of organic PEDOT:PSS devices in air has been noted to be the adsorption of water from the atmosphere.[47] In PEDOT:PSS, the polycationic PEDOT chains are interspersed in the polyanionic poly(4-styrenesulfonate) (PSS) matrix, making it water dispersible. However, the presence of the PSS renders the material to be hygroscopic. This degradation of the PEDOT:PSS layer is spatially inhomogeneous and related with the formation of insulating patches causing a loss of device current, an increase in the resistivity, and consequently a decrease in device efficiency.[48]

While the calibration curve in Figure 3 was obtained under fully hydrated conditions, the effect of humidity on the conductivity of the temperature sensor was estimated by measuring the $I-V$ characteristics while the relative humidity level was varied from 10 to 90%. Further, the effect of sheathing of the sensing layers using a photofibroin layer (top layer shown in Figure 2b) in order to enhance the stability toward humidity was studied. Unsheathed devices and devices using a PTFE tape as the protective sheath were compared. In the devices without a photofibroin passivation layer (unsheathed), the resistance of the sensor was relatively unchanged until ∼60% RH. However, the resistance increased by 6 and 11% upon increasing the humidity level to 70 and 90%, respectively (Figure S6). However, when a photofibroin layer was introduced, the resistance of the sensors increased by only ∼1.2% even under high-humidity (90% RH) conditions (Figure 4a). This is similar to that obtained with PTFE passivation. In contrast, since PTFE is itself nondegradable, it is notable that a degradable fibroin encapsulation/sheath provides excellent protection against humidity interference while enhancing stability in wet environments.

The characteristics of the temperature sensors for heating and cooling cycles were measured. The response of the devices for heating and cooling is similar with a very small hysteresis between the heating and cooling curves. The TCR of the device while heating (−0.989% $°C^{-1}$) was very close to the coefficient on cooling (−0.973% $°C^{-1}$) (Figure 4b). This

https://dx.doi.org/10.1021/acsaelm.0c01017
ACS Appl. Electron. Mater. 2021, 3, 21−29

suggests that the reported temperature sensor can be used in multiple heating and cooling cycles. Indeed, the sensors displayed excellent cycling stability over multiple heating cooling cycles. Only minuscule changes in response were observed over even 50 cycles of consecutive heating and cooling, demonstrating the exceptional consistency of the sensors (Figure 4c). This suggests that the reported temperature sensor can be used in multiple heating and cooling cycles without compromising on precision.

Application of the Sensor for Measuring Surface Temperatures. The ability to detect surface temperature, especially on the human body, reliably in a flexible and conformable format finds potential applications in healthcare, disease diagnostics, and in developing e-skins. As seen in Figure 2a, the sensors are conformable and can be easily applied to complex surfaces including skin and wrinkled fabric. The experiments noted in the prior section were performed using a water bath to maintain a steady and measurable temperature. The response of the flexible sensors was tested in contact with surface temperatures, including human skin. In the first series of experiments, a flexible, soft, synthetic skin surface (commercially available silicone matrix product) was used. A temperature calibration in the range of 23 to 45 °C was used. The synthetic skin slab was immersed in a water bath (40 °C) until an equilibrium temperature was reached. The skin slab was removed, and the sensor was placed on it to obtain the current response. From the calibration plot, the temperature was calculated to be 39.4 °C, which was extremely close to the surface temperature of 39 °C as measured by two different commercial thermometers.

The developed temperature sensor was subsequently deployed on skin for measuring the surface temperature. The conformable nature of the sensor allows it to be easily placed on the forearm surface (Figure 2a). After a reading was taken at room temperature (23 °C, 60% RH), the sensor was placed on the arm, and the response was monitored. The current signal response is practically instantaneous, as the sensor was placed on the skin and stabilized once the skin temperature was reached (Figure 4d). The current signal at the skin temperature was taken for 50 s, with the sensor giving a stable response for the entire duration. Once the sensor was removed from the skin, the current value dropped back to the signal observed at room temperature observed initially. The temperature reading of skin obtained from the calibration curve previously generated was calculated to be 30.4 °C. For the purpose of validation, the skin temperature was measured using a commercial IR skin thermometer, which gave a reading of 30.5 °C. While the skin temperature is below the normal physiological temperature, it may be noted that this temperature is consistent with a forearm skin temperature expected under these ambient conditions.[49] The agreement in temperature response illustrates the fidelity of the sensor developed in this work. The response time of the sensor is notable. From the current vs time graph, an increase in current signal is observed as soon as the sensor was placed on skin, showing that this flexible sensor is rapid and conformable to the underlying surface. It may be noted that the biocompatible fibroin substrate, through which the conduction occurs, is in contact with the surface, rendering it useful for soft interfacial measurements. The application of the sensor for touch detection was also considered. A current response was recorded as soon as a finger was placed on the sensor, indicating its utility for flexible touch panels using an array of sensors.

Flexibility and conformability against soft curvilinear surfaces are two basic requirements for sensors designed for applications on the human body. As shown above, these sensors are easily placed and function on nonrigid and nonplanar surfaces. It is further important to measure the retention of electrical and mechanical properties under nonplanar deformations. We studied the effect of bending on the electrical properties of the sensors by subjecting them to 30, 60, and 90° bends, which may be encountered in the body. The resistance of the sensor under different bend conditions was compared to the resistance of a "flat" sensor. At small bends, no change in the resistance is noted. Even at a 90° bending angle, the resistance increased by only 2.4%, showing the high stability of this device (Figure 5). Importantly, the

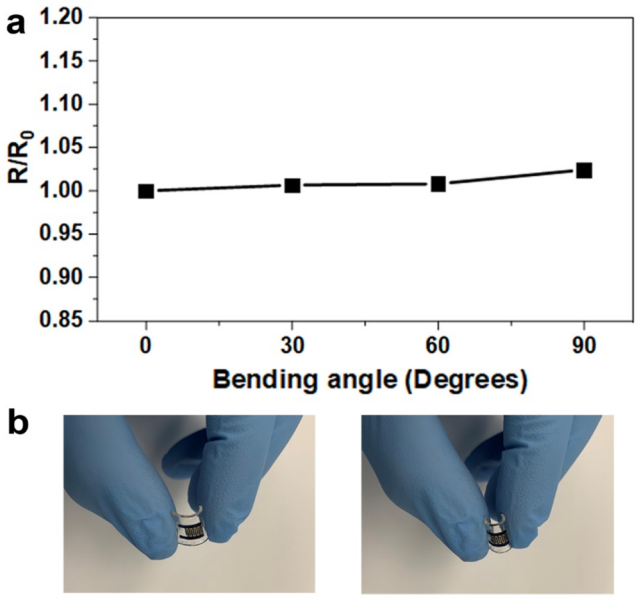

Figure 5. Response of the temperature sensor to bending. The resistance (a) was measured by generating $I-V$ curves at different bends. Representative bending (b) is shown by placing the sensors on a PDMS support that can be flexed.

sensor retains its structural integrity when subjected to mechanical deformations, without any structural failures such as delamination of the electrodes, fracture, or cracking of the layers. Collectively, these experiments demonstrate the utility of the proposed sensor for real-time and continuous monitoring of temperature of arbitrary, dynamic surfaces including soft tissue interfaces.

Degradation Studies. One of the primary advantages of using an organic, biomaterial-based fabrication strategy is the ability to form a degradable device. While the applications demonstrated above are primarily *ex vivo* (e.g., on skin), this property can permit the sensor to be bioresorbed or disappear in a physiological microenvironment after a stable operation lifetime. Silk proteins are known to be enzymatically degraded,[38,50] and various devices shown by our group also possess the ability to be proteolytically degraded over a period of several weeks.[45] A simulation of enzymatic degradation of the temperature sensors was carried out *in vitro* to demonstrate their transient nature. The devices were immersed in a 3.5 U/mL solution of protease at 37 °C. The control consisted of

https://dx.doi.org/10.1021/acsaelm.0c01017
ACS Appl. Electron. Mater. 2021, 3, 21−29

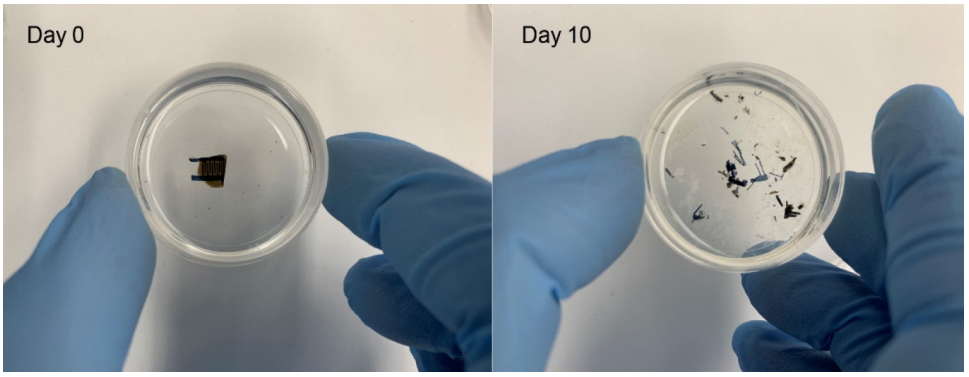

Figure 6. Degradation of the flexible temperature sensor in 10 days in an enzymatic (protease) environment.

devices immersed in 1 M PBS buffer. In the presence of the enzyme, the devices lose their structural integrity in a few days and break apart completely in ∼10 days (Figure 6). It may be noted that in these experiments, a higher protease concentration was employed to accelerate this process. This implies that a sensor in a standard environment can be designed to last longer. A lower protease concentration of 1 U/mL was studied, resulting in proteolytic degradation over 1 month (Figure S7). Similarly, by controlling the thickness of the substrates and the degree of cross-linking, this degradation rate may be further modulated to a period of several weeks. It must be noted that the devices in the control group retain their structural integrity and function, even after 1 month of immersion in buffer. We note that in these experiments, it is the supportive matrix (silk fibroin and sericin) that degrades in the presence of protease enzyme. While PEDOT:PSS and rGO are not known to be degradable inside the human body, the loss of the sericin ink matrix results in their dispersal in the form of fine particles (Figure S7) that can be eventually expelled. We can therefore envision such flexible and degradable devices to be used for short periods of time, in external operation (on body or in textiles) or *in vivo*.

CONCLUSION

In summary, a flexible silk/PEDOT:PSS device is shown for the monitoring of surface temperature. The device is a fully organic, degradable temperature sensor that possesses several useful features including a small size with high-resolution, reproducible microstructured electrodes. The entire device is optically transparent, mechanically robust while being flexible and conformable to complex surfaces. Notably, this sensor is formed from protein matrices that comprise an organic framework for the device while allowing it to be proteolytically degraded over a period of several weeks. The sensing performance was stable against humidity variations while being able to function in fully hydrated environments. The sensor response is rapid, repeatable, and cyclable and functions under various mechanical challenges. Such systems may be applied for wearable and degradable applications for on-body, tissue interfacing, implantable physiological monitoring of temperature or as e-skins that can provide a temperature response to touch.

ASSOCIATED CONTENT

Supporting Information

The Supporting Information is available free of charge at https://pubs.acs.org/doi/10.1021/acsaelm.0c01017.

SEM images of the cross section of the sensor; *I*−*V* curves as a function of temperature; temperature sensitivity comparisons of individual composites with the final sensor; comparison of the effect of rGO in ink vs the top layer; effect of rGO concentration on temperature response; effect of RH on resistance without fibroin encapsulation; enzymatic degradation of the sensor over 4 weeks (PDF)

AUTHOR INFORMATION

Corresponding Author

Vamsi K. Yadavalli − *Department of Chemical and Life Science Engineering, Virginia Commonwealth University, Richmond, Virginia 23284, United States;* orcid.org/0000-0002-8879-1948; Phone: 1-804-828-0587; Email: vyadavalli@vcu.edu

Author

Sayantan Pradhan − *Department of Chemical and Life Science Engineering, Virginia Commonwealth University, Richmond, Virginia 23284, United States*

Complete contact information is available at: https://pubs.acs.org/10.1021/acsaelm.0c01017

Notes

The authors declare no competing financial interest.

ACKNOWLEDGMENTS

This research was supported in part by funding from the National Science Foundation (CBET-1704435). V.K.Y. acknowledges support from the CCI Central VA Node. SEM images were obtained at the VCU Nanomaterials Characterization Center.

REFERENCES

(1) Feig, V. R.; Tran, H.; Bao, Z. Biodegradable polymeric materials in degradable electronic devices. *ACS Cent. Sci.* **2018**, *4* (3), 337−348.
(2) Pradhan, S.; Brooks, A. K.; Yadavalli, V. K. Nature-derived materials for the fabrication of functional biodevices. *Mater. Today Bio* **2020**, *7*, 100065.
(3) Irimia-Vladu, M. Green" electronics: biodegradable and biocompatible materials and devices for sustainable future. *Chem. Soc. Rev.* **2014**, *43* (17), 588.
(4) Li, W.; Liu, Q.; Zhang, Y.; Li, C. a.; He, Z.; Choy, W. C.; Low, P. J.; Sonar, P.; Kyaw, A. K. K. Biodegradable materials and green processing for green electronics. *Adv. Mater.* **2020**, *32* (33), 2001591.
(5) Kang, S.; Yin, L.; Bettinger, C. The emergence of transient electronic devices. *MRS Bull.* **2020**, *45* (2), 87−95.

(6) Singh, R.; Bathaei, M. J.; Istif, E.; Beker, L. A Review of Bioresorbable Implantable Medical Devices: Materials, Fabrication, and Implementation. *Adv. Healthcare Mater.* **2020**, *9*, 2000790.
(7) Li, C.; Guo, C.; Fitzpatrick, V.; Ibrahim, A.; Zwierstra, M. J.; Hanna, P.; Lechtig, A.; Nazarian, A.; Lin, S. J.; Kaplan, D. L. Design of biodegradable, implantable devices towards clinical translation. *Nat. Rev. Mater.* **2020**, *5*, 61.
(8) Youn, D.-Y.; Jung, U.; Naqi, M.; Choi, S.-J.; Lee, M.-G.; Lee, S.; Park, H.-J.; Kim, I.-D.; Kim, S. Wireless real-time temperature monitoring of blood packages: silver nanowire-embedded flexible temperature sensors. *ACS Appl. Mater. Interfaces* **2018**, *10* (51), 44678−44685.
(9) Dang, B.; Wu, Q.; Song, F.; Sun, J.; Yang, M.; Ma, X.; Wang, H.; Hao, Y. A bio-inspired physically transient/biodegradable synapse for security neuromorphic computing based on memristors. *Nanoscale* **2018**, *10* (43), 20089−20095.
(10) Ray, T. R.; Choi, J.; Bandodkar, A. J.; Krishnan, S.; Gutruf, P.; Tian, L.; Ghaffari, R.; Rogers, J. A. Bio-integrated wearable systems: a comprehensive review. *Chem. Rev.* **2019**, *119* (8), 5461−5533.
(11) Kuzubasoglu, B. A.; Bahadir, S. K. Flexible Temperature Sensors: A Review. *Sens. Actuators, A* **2020**, *315*, 112282.
(12) Li, Q.; Zhang, L. N.; Tao, X. M.; Ding, X. Review of flexible temperature sensing networks for wearable physiological monitoring. *Adv. Healthcare Mater.* **2017**, *6* (12), 1601371.
(13) Chen, Y.; Lu, B.; Chen, Y.; Feng, X. Breathable and stretchable temperature sensors inspired by skin. *Sci. Rep.* **2015**, *5*, 11505.
(14) Dan, L.; Elias, A. L. Flexible and Stretchable Temperature Sensors Fabricated Using Solution-Processable Conductive Polymer Composites. *Adv. Healthcare Mater.* **2020**, *9*, 2000380.
(15) Liu, Q.; Tai, H.; Yuan, Z.; Zhou, Y.; Su, Y.; Jiang, Y. A High-Performances Flexible Temperature Sensor Composed of Polyethyleneimine/Reduced Graphene Oxide Bilayer for Real-Time Monitoring. *Adv. Mater. Technol.* **2019**, *4* (3), 1800594.
(16) Kim, J.; Campbell, A. S.; de Ávila, B. E.-F.; Wang, J. Wearable biosensors for healthcare monitoring. *Nat. Biotechnol.* **2019**, *37* (4), 389−406.
(17) Salvatore, G. A.; Sülzle, J.; Dalla Valle, F.; Cantarella, G.; Robotti, F.; Jokic, P.; Knobelspies, S.; Daus, A.; Büthe, L.; Petti, L.; et al. Biodegradable and highly deformable temperature sensors for the internet of things. *Adv. Funct. Mater.* **2017**, *27* (35), 1702390.
(18) Yuvaraja, S.; Nawaz, A.; Liu, Q.; Dubal, D.; Surya, S. G.; Salama, K. N.; Sonar, P. Organic field-effect transistor-based flexible sensors. *Chem. Soc. Rev.* **2020**, *49*, 3423−3460.
(19) Jung, S.; Ji, T.; Varadan, V. K. Point-of-care temperature and respiration monitoring sensors for smart fabric applications. *Smart Mater. Struct.* **2006**, *15* (6), 1872.
(20) Khan, M. R. R.; Kang, S. Fast, Highly Sensitive Interdigitated Capacitor Sensor to Detect Wide Range of Temperatures Using Graphene-Oxide-Containing Dielectric Membrane. *IEEE Sens. J.* **2018**, *18* (7), 2667−2674.
(21) Fan, X.; Nie, W.; Tsai, H.; Wang, N.; Huang, H.; Cheng, Y.; Wen, R.; Ma, L.; Yan, F.; Xia, Y. PEDOT: PSS for flexible and stretchable electronics: modifications, strategies, and applications. *Adv. Sci.* **2019**, *6* (19), 1900813.
(22) Kanao, K.; Harada, S.; Yamamoto, Y.; Honda, W.; Arie, T.; Akita, S.; Takei, K. Highly selective flexible tactile strain and temperature sensors against substrate bending for an artificial skin. *RSC Adv.* **2015**, *5* (38), 30170−30174.
(23) Yu, Y.; Peng, S.; Blanloeuil, P.; Wu, S.; Wang, C. H. Wearable Temperature Sensors with Enhanced Sensitivity by Engineering Microcrack Morphology in PEDOT: PSS−PDMS Sensors. *ACS Appl. Mater. Interfaces* **2020**, *12* (32), 36578−36588.
(24) Vuorinen, T.; Niittynen, J.; Kankkunen, T.; Kraft, T. M.; Mäntysalo, M. Inkjet-Printed Graphene/PEDOT:PSS Temperature Sensors on a Skin-Conformable Polyurethane Substrate. *Sci. Rep.* **2016**, *6* (1), 35289.
(25) Bießmann, L.; Kreuzer, L. P.; Widmann, T.; Hohn, N.; Moulin, J.-F. o.; Müller-Buschbaum, P. Monitoring the Swelling Behavior of PEDOT: PSS electrodes under high humidity conditions. *ACS Appl. Mater. Interfaces* **2018**, *10* (11), 9865−9872.
(26) Wang, Y.-F.; Sekine, T.; Takeda, Y.; Yokosawa, K.; Matsui, H.; Kumaki, D.; Shiba, T.; Nishikawa, T.; Tokito, S. Fully Printed PEDOT:PSS-based Temperature Sensor with High Humidity Stability for Wireless Healthcare Monitoring. *Sci. Rep.* **2020**, *10* (1), 2467.
(27) Cui, C.; Fu, Q.; Meng, L.; Hao, S.; Dai, R.; Yang, J. Recent Progress in Natural Biopolymers Conductive Hydrogels for Flexible Wearable Sensors and Energy Devices: Materials, Structures and Performance. *ACS Appl. Bio Mater.* **2020** ().
(28) Liu, J.; Chen, Q.; Liu, Q.; Zhao, B.; Ling, S.; Yao, J.; Shao, Z.; Chen, X. Intelligent Silk Fibroin Ionotronic Skin for Temperature Sensing. *Adv. Mater. Technol.* **2020**, *5* (7), 2000430.
(29) Wang, C.; Xia, K.; Zhang, M.; Jian, M.; Zhang, Y. An All-Silk-Derived Dual-Mode E-skin for Simultaneous Temperature−Pressure Detection. *ACS Appl. Mater. Interfaces* **2017**, *9* (45), 39484−39492.
(30) Wang, Q.; Ling, S.; Liang, X.; Wang, H.; Lu, H.; Zhang, Y. Self-healable multifunctional electronic tattoos based on silk and graphene. *Adv. Funct. Mater.* **2019**, *29* (16), 1808695.
(31) Kurland, N. E.; Dey, T.; Kundu, S. C.; Yadavalli, V. K. Precise Patterning of Silk Microstructures Using Photolithography. *Adv. Mater.* **2013**, *25* (43), 6207−6212.
(32) Kurland, N. E.; Dey, T.; Wang, C.; Kundu, S. C.; Yadavalli, V. K. Silk Protein Lithography as a Route to Fabricate Sericin Microarchitectures. *Adv. Mater.* **2014**, *26* (26), 4431.
(33) Feiner, R.; Dvir, T. Tissue−electronics interfaces: From implantable devices to engineered tissues. *Nat. Rev. Mater.* **2018**, *3* (1), 17076.
(34) Muskovich, M.; Bettinger, C. J. Biomaterials-Based Electronics: Polymers and Interfaces for Biology and Medicine. *Adv. Healthcare Mater.* **2012**, *1* (3), 248−266.
(35) Pal, R. K.; Farghaly, A. A.; Collinson, M. M.; Kundu, S. C.; Yadavalli, V. K. Photolithographic Micropatterning of Conducting Polymers on Flexible Silk Matrices. *Adv. Mater.* **2016**, *28* (7), 1406−1412.
(36) Zhang, J.; Yang, H.; Shen, G.; Cheng, P.; Zhang, J.; Guo, S. Reduction of graphene oxide vial-ascorbic acid. *Chem. Commun.* **2010**, *46* (7), 1112−1114.
(37) Pal, R. K.; Kundu, S. C.; Yadavalli, V. K. Fabrication of flexible, fully organic, degradable energy storage devices using silk proteins. *ACS Appl. Mater. Interfaces* **2018**, *10* (11), 9620−9628.
(38) Brenckle, M. A.; Cheng, H.; Hwang, S.; Tao, H.; Paquette, M.; Kaplan, D. L.; Rogers, J. A.; Huang, Y.; Omenetto, F. G. Modulated Degradation of Transient Electronic Devices through Multilayer Silk Fibroin Pockets. *ACS Appl. Mater. Interfaces* **2015**, *7* (36), 19870−19875.
(39) Zhou, Z. T.; Zhang, S. Q.; Cao, Y. T.; Marelli, B.; Xia, X. X.; Tao, T. H. Engineering the Future of Silk Materials through Advanced Manufacturing. *Adv. Mater.* **2018**, *30* (33), 1706983.
(40) Tao, H.; Kaplan, D. L.; Omenetto, F. G. Silk Materials - A Road to Sustainable High Technology. *Adv. Mater.* **2012**, *24* (21), 2824−2837.
(41) Kim, D. H.; Viventi, J.; Amsden, J. J.; Xiao, J. L.; Vigeland, L.; Kim, Y. S.; Blanco, J. A.; Panilaitis, B.; Frechette, E. S.; Contreras, D.; Kaplan, D. L.; Omenetto, F. G.; Huang, Y. G.; Hwang, K. C.; Zakin, M. R.; Litt, B.; Rogers, J. A. Dissolvable films of silk fibroin for ultrathin conformal bio-integrated electronics. *Nat. Mater.* **2010**, *9* (6), 511−517.
(42) Zhou, J.; Anjum, D. H.; Chen, L.; Xu, X.; Ventura, I. A.; Jiang, L.; Lubineau, G. The temperature-dependent microstructure of PEDOT/PSS films: insights from morphological, mechanical and electrical analyses. *J. Mater. Chem. C* **2014**, *2* (46), 9903−9910.
(43) Vitoratos, E.; Sakkopoulos, S.; Dalas, E.; Paliatsas, N.; Karageorgopoulos, D.; Petraki, F.; Kennou, S.; Choulis, S. A. Thermal degradation mechanisms of PEDOT: PSS. *Org. Electron.* **2009**, *10* (1), 61−66.
(44) Xu, M.; Pradhan, S.; Agostinacchio, F.; Pal, R. K.; Greco, G.; Mazzolai, B.; Pugno, N. M.; Motta, A.; Yadavalli, V. K. Easy, Scalable,

Robust, Micropatterned Silk Fibroin Cell Substrates. *Adv. Mater. Interfaces* **2019**, *6* (8), 1801822.
(45) Xu, M.; Yadavalli, V. K. Flexible biosensors for the impedimetric detection of protein targets using silk-conductive polymer biocomposites. *ACS Sens.* **2019**, *4* (4), 1040−1047.
(46) Kuş, M.; Okur, S. Electrical characterization of PEDOT: PSS beyond humidity saturation. *Sens. Actuators, B* **2009**, *143* (1), 177−181.
(47) Kawano, K.; Pacios, R.; Poplavskyy, D.; Nelson, J.; Bradley, D. D.; Durrant, J. R. Degradation of organic solar cells due to air exposure. *Sol. Energy Mater. Sol. Cells* **2006**, *90* (20), 3520−3530.
(48) Huang, J.; Miller, P. F.; Wilson, J. S.; de Mello, A. J.; de Mello, J. C.; Bradley, D. D. Investigation of the effects of doping and post-deposition treatments on the conductivity, morphology, and work function of poly (3, 4-ethylenedioxythiophene)/poly (styrene sulfonate) films. *Adv. Funct. Mater.* **2005**, *15* (2), 290−296.
(49) Yao, Y.; Lian, Z.; Liu, W.; Shen, Q. Experimental study on skin temperature and thermal comfort of the human body in a recumbent posture under uniform thermal environments. *Indoor Built Environ.* **2007**, *16* (6), 505−518.
(50) Horan, R. L.; Antle, K.; Collette, A. L.; Wang, Y. Z.; Huang, J.; Moreau, J. E.; Volloch, V.; Kaplan, D. L.; Altman, G. H. In vitro degradation of silk fibroin. *Biomaterials* **2005**, *26* (17), 3385−3393.
(51) Wang, Q.; Ling, S.; Liang, X.; Wang, H.; Lu, H.; Zhang, Y. Self-Healable Multifunctional Electronic Tattoos Based on Silk and Graphene. *Adv. Funct. Mater.* **2019**, *29* (16), 1808695.
(52) Yu, Y.; Peng, S.; Blanloeuil, P.; Wu, S.; Wang, C. H. Wearable Temperature Sensors with Enhanced Sensitivity by Engineering Microcrack Morphology in PEDOT:PSS−PDMS Sensors. *ACS Appl. Mater. Interfaces* **2020**, *12*, 36578.
(53) Zhang, F.; Hu, H.; Islam, M.; Peng, S.; Wu, S.; Lim, S.; Zhou, Y.; Wang, C.-H. Multi-modal strain and temperature sensor by hybridizing reduced graphene oxide and PEDOT:PSS. *Compos. Sci. Technol.* **2020**, *187*, 107959.

https://dx.doi.org/10.1021/acsaelm.0c01017
ACS Appl. Electron. Mater. 2021, 3, 21−29